

**STUDY ON THE EFFECTS OF ALTERNATIVE-KEROSENE  
FUEL MIXTURE ON COMBUSTION SPRAY  
CHARACTERISTICS FOR DIFFERENT SPRAY HALF  
CONE ANGLE**

**FARAH SYAFIQAH BINTI ROSLAN**

**SCHOOL OF AEROSPACE ENGINEERING  
UNIVERSITI SAINS MALAYSIA**

**2018**

**STUDY ON THE EFFECTS OF ALTERNATIVE-KEROSENE FUEL MIXTURE  
ON COMBUSTION SPRAY CHARACTERISTICS FOR DIFFERENT SPRAY  
HALF CONE ANGLE**

**by**

**FARAH SYAFIQAH BINTI ROSLAN**

**Thesis submitted in fulfillment of the requirements for the Bachelor Degree of  
Engineering (Honours) (Aerospace Engineering)**

**June 2018**

## ENDORSEMENT

I, Farah Syafiqah Binti Roslan, hereby declare that all corrections and comments made by the supervisor and examiner have been taken consideration and rectified accordingly.

---

(Signature of Student)

Date :

---

(Signature of Supervisor)

Name :

Date :

---

(Signature of Examiner)

Name :

Date :

## DECLARATION

This thesis is the result of my own investigation, except where otherwise stated and has not previously been accepted in substance for any degree and is not being concurrently submitted in candidature for any other degree.

---

(Signature of Student)

Date :

## ACKNOWLEDGEMENTS

First and foremost, thank you Allah for His blessings.

I would like to express my gratitude and appreciation to my supervisor and lecturer, Dr. Nurul Musfirah Mazlan for her continuous assistance and dedicated involvement in every step throughout my final year project. Her advice and knowledge had helped me in completing my final year project and getting through my studies years.

None of this could have happened without my family. My parents, Roslan Kidam and Zahrah Md. Ramli, have always been my motivation and my sisters have been nothing but very supportive every time I told them I feel like giving up throughout these four years of studies. Thank you for always having faith in me.

I would also like to thank my friends, Amira Syuhadah, Rahmah, Nurhamizah and my other classmates for their help, for their friendship, for always listening to my problems and for tolerating me throughout the years. Without their supportive words and company, I would go through the four years of study alone and in constant doubt.

Lastly, I would like to express my gratitude to all the lecturers and teachers that have taught me for the last four years. The knowledge that they shared will be pass on to the next generations and their wise words will always give an impact in my life to become a better person than I am today.

**STUDY ON THE EFFECTS OF ALTERNATIVE-KEROSENE FUEL MIXTURE  
ON COMBUSTION SPRAY CHARACTERISTICS FOR DIFFERENT SPRAY  
HALF CONE ANGLE**

**ABSTRACT**

This study focuses on simulating a two-dimensional (2D) case of a simple cylindrical combustion chamber to study the effects of alternative-kerosene fuel mixture on combustion spray characteristics for different spray half cone angles. The simulation is performed by using Computational Fluid Dynamic (CFD). The fuels that are used for the simulation are Jet-A, Jatropa Bio-synthetic Paraffinic Kerosene (JSPK), and Camelina Bio-synthetic Paraffinic Kerosene (CSPK). Additionally, the mixture of 50% JSPK with 50% Jet-A (50JSPK/50Jet-A) and the mixture of 50% CSPK with 50% Jet-A (50CSPK/50Jet-A) are used to examine the effects of blend fuel. Every fuel is simulated at 30°, 40° and 50° of injection spray half cone angle. The velocity of the fuel injection spray is considered in X and Y direction. The results obtained is compared in terms of the temperature profile, spray penetration and injection discrete particle model evaporation. From the simulation, it is found that as the spray half cone angle increases, the distance of the maximum temperature increases, the final temperature increase, the time taken for droplet to evaporate increases and discrete phase model evaporation decreases. At 40° and 50° spray half cone angle, Jet-A has the shortest time taken to completely evaporate and highest DPM evaporation which is then followed by 50JSPK/50Jet-A, 50CSPK/50Jet-A, JSPK and CSPK. Furthermore, Jet-A has the shortest distance to completely evaporate and it is followed by JSPK, 50CSPK/50Jet-A, 50JSPK/50Jet-A and CSPK.

**KAJIAN MENGENAI KESAN CAMPURAN BAHAN BAKAR ALTERNATIF-  
KEROSIN KE ATAS CIRI-CIRI PERCIKAN PEMBAKARAN BAHAN BAKAR  
BAGI SUDUT PERCIKAN SEPARUH KON YANG BERLAINAN**

**ABSTRAK**

Kajian ini bertujuan untuk menjalankan sebuah dua dimensi (2D) simulasi bagi kebuk pembakaran berbentuk silinder biasa untuk mengkaji kesan-kesan campuran bahan bakar alternative-kerosin ke atas ciri-ciri percikan pembakaran bagi sudut percikan separuh kon yang berbeza. Simulasi ini dijalankan dengan menggunakan Komputasi Dinamik Bendalir (CFD). Bahan bakar yang digunakan untuk simulasi ini adalah Jet-A, Jatropha Bio-synthetic Paraffinic Kerosene (JSPK), dan Camelina Bio-synthetic Paraffinic Kerosene (CSPK). Tambahan pula, campuran bahan bakar 50% JSPK bersama 50% Jet-A (50JSPK/50Jet-A) dan campuran bahan bakar 50% CSPK bersama 50% Jet-A (50CSPK/50Jet-A) digunakan untuk mengkaji kesan terhadap bahan bakar campuran. Simulasi ini dijalankan pada sudut percikan separuh kon 30°, 40° dan 50°. Kelajuan percikan bahan bakar mengambil kira kelajuan pada arah paksi X dan Y. Keputusan yang diperoleh akan dibandingkan daripada segi profil suhu, penyejatan percikan, dan penyejatan model fasa diskret (DPM). Daripada simulasi tersebut, didapati bahawa apabila sudut percikan separuh kon meningkat, jarak untuk suhu maksima meningkat, suhu akhir meningkat, masa yang diambil untuk percikan menyejatkan meningkat dan penyejatan model fasa diskret menurun. Pada sudut percikan 40° dan 50°, Jet-A mengambil masa paling singkat untuk disejatkan sepenuhnya dan penyejatan DPM yang paling tinggi dan ianya diikuti oleh 50JSPK/50Jet-A, 50CSPK/50Jet-A, JSPK dan CSPK. Selain itu, Jet-A mempunyai

jarak paling pendek untuk disejat sepenuhnya kemudian diikuti oleh JSPK, 50CSPK/50Jet-A, 50JSPK/50Jet-A dan CSPK.

## TABLE OF CONTENTS

<b>DECLARATION</b>	ii
<b>ACKNOWLEDGEMENTS</b>	iii
<b>ABSTRACT</b>	iv
<b>ABSTRAK</b>	v
<b>LIST OF FIGURES</b>	ix
<b>LIST OF TABLES</b>	xi
<b>LIST OF ABBREVIATIONS</b>	xii
<b>LIST OF SYMBOLS</b>	xiii
<b>CHAPTER</b>	
<b>1 INTRODUCTION</b>	1
1.1 General Introduction and Problem Statement	1
1.2 Objectives	4
1.3 Thesis Outline	4
1.4 Expected Contribution of Knowledge	5
<b>2 LITERATURE REVIEW</b>	6
<b>3 METHODOLOGY</b>	11
3.1 Flow Chart	11
3.2 Fuels Properties	12
3.3 Combustion Chamber Configuration	14
3.4 Combustion Chamber Zones	15
3.5 Meshing of the Combustion Chamber	17
3.6 CFD Modeling: Non-premixed Combustion	19
3.7 CFD Modeling: Discrete Phase Model	19
3.8 Boundary Conditions	22
3.9 CFD Solution Methods	24
3.10 CFD Solution Control, Initialization and Calculation	24
3.11 Simulation Validation	25

<b>4</b>	<b>RESULTS AND DISCUSSION</b>	27
4.1	Maximum Temperature and Distance	27
4.2	Flame Temperature	32
4.3	Drop Size Evaporation against Time	35
4.4	Drop Size Evaporation against Distance	41
4.5	Discrete Phase Modeling Evaporation	46
<b>5</b>	<b>CONCLUSION AND RECOMMENDATIONS</b>	50
	<b>REFERENCES</b>	53
	<b>APPENDICES</b>	56
	A - Combustion Chamber Temperature Profile	56
	B - Temperature for Alternative Fuels along the Combustion Chamber	62
	C - Discrete Particle Model Evaporation (DPM)	64

## LIST OF FIGURES

Figure 3.1: Methodology flowchart	11
Figure 3.2: Combustion chamber configuration (Jafarinia, 2017). The dimensions are in meter.	14
Figure 3.3: Combustion zones for the combustion chamber.	16
Figure 3.4: Meshing for the half upper part of the combustion chamber.	18
Figure 3.5: Close up view of the meshing.	18
Figure 3.6: Drop velocity representation in X and Y directions.	20
Figure 3.7: Percentage difference between CFD simulation and study by Azami and Savill for Jet-A at 34.89° spray half cone angle (Azami and Savill, 2016).	25
Figure 4.1: Temperature contour along the combustion chamber for Jet-A at spray half cone angle of 30°, 40° and 50° respectively.	28
Figure 4.2: Temperature for Jet-A at different spray half cone angle along the combustion chamber.	30
Figure 4.3: The distance from injector where the maximum temperature is achieved for different type of fuel at different spray half cone angle.	31
Figure 4.4: Flame temperature at different spray half cone angle for different type of fuels.	32
Figure 4.5: Percentage difference for flame temperature at different spray half cone angle for all type of fuels.	33
Figure 4.6: Particles diameter distribution for Jet-A at 30° spray half cone angle.	35
Figure 4.7: Time taken for particle penetration at different spray half cone angle for Jet-A.	36
Figure 4.8: Maximum time taken for particle to evaporate at different spray half cone angle.	37
Figure 4.9: Maximum time taken for particle to evaporate for different type of fuel.	37
Figure 4.10: Time taken for particle penetration percentage difference at different spray half cone angle for different type of fuel.	39
Figure 4.11: Distance where particle starts to evaporate	41

Figure 4.12: Maximum distance for particle to evaporate at different spray half cone angle.	42
Figure 4.13: Maximum distance for particle to evaporate for different type of fuel.	43
Figure 4.14: Percentage difference of maximum distance for particle evaporation at different spray half cone angle for different type of fuel.	44
Figure 4.15: Discrete phase modeling evaporation for Jet-A at 30°, 40° and 50° respectively.	47
Figure 4.16: Maximum DPM evaporation at different spray half cone angle for different type of fuel.	48
Figure 4.17: Percentage difference for maximum DPM evaporation.	48

## LIST OF TABLES

Table 3.1: Fuel properties (Mazlan, 2012, Azami and Savill, 2016).	12
Table 3.2: Combustion zones length in the combustion chamber from the journal (Mark and Selwyn, 2016).	15
Table 3.3: Combustion zones length in the combustion chamber for cylindrical combustion chamber.	16
Table 3.4: Combustion chamber's mesh quality.	17
Table 3.5: X and Y velocity for every spray half cone angle.	20
Table 3.6: Particle injection properties.	21
Table 3.7: Inlet boundary conditions.	22
Table 3.8: Outlet boundary conditions.	23
Table 3.9: Wall boundary conditions.	23

## LIST OF ABBREVIATIONS

CFD	: Computational Fluid Dynamics
NO <sub>x</sub>	: Nitrogen Oxide
C <sub>12</sub> H <sub>23</sub>	: Chemical formula for kerosene
DPM	: Discrete Phase Model
JSPK	: Jatropa Bio-synthetic Paraffinic Kerosene
CSPK	: Camelina Bio-synthetic Paraffinic Kerosene
50JSPK/50Jet-A	: Mixture of 50% JSPK with 50% Jet-A
50CSPK/50Jet-A	: Mixture of 50% CSPK with 50% Jet-A
PDF	: Probability Density Function

## LIST OF SYMBOLS

$P_{sat}$	:	Saturation pressure [Pa]
$T_p$	:	Droplet particle temperature [K]
$c_p$	:	Specific heat [ $J/kgK$ ]
$\rho$	:	Density [ $kg/m^3$ ]
$x$	:	Fuel percentage [%]
$i$	:	Type of fuel
$\theta$	:	Spray half cone angle [ $^\circ$ ]

# **CHAPTER 1**

## **INTRODUCTION**

This chapter provides a general introduction describing problem statement to the case study, objectives of the case study, thesis outline and the expected contribution of knowledge.

### **1.1 General Introduction and Problem Statement**

Air transport acquired a significant role in the everyday life of modern world. The influence of air travel increased worldwide social contact, especially in improving business and marketing (Kandaramath Hari et al., 2015). Emissions resulting from the combustion of fossil fuels are usually considered as the main responsible for greenhouse gas emissions. It is found that 3% of European Union greenhouse gas emissions are from aviation industry. Furthermore, aviation is the only direct source of emissions into the upper atmosphere (Oliveira and Brójo, 2017). The total diesel fuel and jet fuel consumption was in the range of 5 to 6 million barrels per day in between 2005 to 2010 (André Faaij 2012). In order to achieve a greener world for future generations, it is important for researchers and engineers to find a solution to reduce the current pollution problem that we are having.

Gas turbine engines are commonly used for most aircrafts especially big civil aircrafts such as Airbus A330, Boeing 737 and many more. It is known that kerosene is the main fuel for powering an aircraft's engine. There are many types of fuel that is used depends on the purpose of the aircraft. Civil aircraft usually use fuel like Jet-A1, Jet-A and Jet-B (Shell.com, 2018b) while military aircrafts use fuel like JP-4, JP-8 and JP-5 (Shell.com, 2018d). Small piston engines aircrafts are usually used for flying club, flight training, crops spraying and private pilots. These aircrafts can be powered up by using gasoline which is also known as Avgas. There are also a few types of Avgas such as Avgas 100 and Avgas 100LL (Shell.com, 2018a).

In order to help reducing the emissions that are produced by the aircraft's engines, there are a few solutions that can be considered. The performance of the fuel that are currently available in the market can be improved or by finding other alternative fuels that produce less pollution.

Studies on alternative fuel have been conducted immensely. For instance Azami et al. have conducted a computational study to evaluate evaporation and spray penetration of different alternative fuels (Azami and Savill, 2016). However, the simulation only considered the fuel to be flowing in zero-dimension, where the particle velocity was only considered in one direction which is in the X direction. The simulation was also run for different initial temperature and initial velocity only. In addition, the alternative fuels that were used were pure biofuel instead of mixture with kerosene.

An experiment conducted by Zhang T. et al. used different nozzles diameter of pressure-swirl atomizer to study the effects of it on spray characteristics at different injection pressure (Zhang et al., 2017). However, they only considered the results on how different nozzles diameter affect the spray cone angle. The results did not include on how the different nozzles diameter affect the penetration or evaporation of the fuel.

Another CFD simulations to study the effects of fuel physical properties on direct injection spray and ignition behavior were conducted by Kim et al. (Kim et al., 2016). From this study, the results indicate that liquid density, specific heat, viscosity and vapor pressure should be considered for surrogate development to properly capture the liquid penetration and ignition delay of the target fuel. However, the results did not mention the effects on the spray cone angle.

The experimental and simulated performance of an Armfield CM4 turbojet engine was investigated by Abu Talib et al. for palm oil methyl ester biodiesel (PME) and its blends with conventional Jet-A1 fuel (Abu Talib et al., 2014). The results that were obtained are in terms of the engine's thrust and thermal efficiency. They did not mention on how the fuel was penetrated inside the engine.

Therefore, this study is conducted to also model the evaporation and spray penetration for alternative fuels and kerosene. The penetration will involve the fuel mixture of alternative fuel-kerosene and kerosene as reference. It will be simulated at different spray half cone angle to see how different half cone angles will affect the penetration of the fuel and the temperature. Other than that, the simulation will also be conducted in two-dimensions where the particle velocity is considered in both X and Y directions.

## **1.2 Objectives**

The objectives of this case study are:

1. To simulate the spray visualization of different type of fuel at different spray half cone angle by using the CFD software;
2. To compare the spray characteristics in terms of temperature profile, injected particle diameter and discrete phase model evaporation for different type of fuel at different spray half cone angle.

## **1.3 Thesis Outline**

This thesis contains five chapters:

- First chapter presents general introduction to this thesis. In this chapter, the problem statement is presented. The objectives for this case study, the thesis outline and the expected contribution of knowledge are also being presented in this chapter.
- Second chapter discusses the literature review. In this chapter, methods that were used by other researchers that did almost similar simulations or experiments will be compared. The results that they obtained from their simulations or experiments can be further discussed and compared to the results of this case study.
- The third chapter discussed about methodology. This chapter is divided into a few subsections which describe on how the simulation is set up starting from the geometry of the combustion chamber, the usage of ANSYS Fluent software, type of meshing for the combustion chamber, the fuel properties that are used, CFD modeling, boundary conditions, CFD solution methods, CFD solution controls, initialization, calculation and validation with simulation from a journal.

- Simulation results such as temperature profile, particle drop evaporation against time and length, and discrete phase model for every type of fuel at different spray half cone angle are discussed in Chapter 4.
- Last chapter concludes present research study. Type of fuel at which spray half cone angle that is suitable to help reduce the emissions and pollution is proposed. Other than that, recommendation of things or steps that can improve simulation will also be included in this chapter. In addition, discussions towards future work that could be done in providing necessary understanding in regards to bio-fuel aspects are presented.

#### **1.4 Expected Contribution of Knowledge**

In this study it is expected to contribute knowledge in term of ideas to manufacturers or other researchers in determining fuel mixture and spray half cone angle that are suitable for greener aviation industry.

## **CHAPTER 2**

### **LITERATURE REVIEW**

This chapter provides state-of-art on previous researches conducted on combustion characteristics.

The performance of the fuel can be improved by adding additives. Additives are added to eliminate undesirable effects or to meet specific requirements of certain aircraft or airline operators. Additives are added in quantities that are often only measurable in parts per million (Shell.com, 2018c). Hydrotreating process is a process to reduce the sulphur active compounds presents in kerosene to elemental sulphur to obtain a jet fuel with sulphur level according to the present directive. This process generates a peroxidation of some hydrocarbons. To avoid peroxide production after the refinery process, a specific antioxidant additive should be added on fuel. (Bernabei et al., 2000).

Researchers also found that biofuels can be a potential replacement for conventional jet fuel. Biofuels can be defined as combustible liquids that are manufactured from renewable sources such as plant crops (Oliveira and Brójo, 2017). Renewable resources that can be produced as alternative aviation fuels include camelina, jatropha, and algae. Camelina is a non-food energy crop with high oil content while jatropha is a non-edible crop which can grow in marginal land. Meanwhile, algae contain high lipids and has high rate of carbon dioxide absorption. Their properties give a few advantages such as reduce the greenhouse gas emission, compatible with conventional fuel, sustainable and produce clean burning (Kandaramath Hari et al., 2015).

A computational fluid dynamics (CFD) simulation was done by Oliveira and Brójo (Oliveira and Brójo, 2017) to simulate burning Jet-A and a 100% blend of biofuels – which are jatropha seeds, algae and sunflower – inside CFM56-3 combustor. CFM56-3 is a type of engine that is manufactured by CFM International and it was developed to incorporate in Boeing 737 (Martins, 2015). A 3D scan had to be performed followed by a CAD design to obtain the accurate model of the combustor due to confidentiality of the combustor's blueprint. Even though the simulation was run by using ANSYS Fluent, the generation of the meshing was performed by using HELYX-OS. The viscous model that was chosen was RSM and for the radiation model, Discrete Ordinate (DO) was chosen. The species model that was chosen was non-premixed combustion. A thermodynamic database was used to determine the thermodynamic properties for the fuel except for Jet-A since it is already available in the software. The simulation was done only for a quarter section of the combustor due to its symmetry. So, for the boundary conditions, the total air, fuel mass flow rates and overall Air Fuel Ratio were divided by four. From the simulation, it is found that algae had the highest reduction of emissions followed by sunflower and jatropha.

CFD simulation can be done to analyze the flow field in the atomizers. Yu et al. did a simulation for a swirl atomizer by applying renormalization group (RNG) k-turbulent model to the numerical solution of the flow field and SIMPLE algorithm was used to solve the finite difference equation (Yu et al., 2012). Another simulation for a plain orifice atomizer (Tan et al., 2017) used realizable k-epsilon turbulence model in order to account for locally transient flow. Kim et al. utilized RNG k-epsilon model to model the turbulence in the gas-phase flow field to study the effects of fuel physical properties on direct injection spray and ignition behavior (Kim et al., 2016). These CFD models can be considered to be used to run the simulation for this case study.

Spray cone angle is defined as an angle formed by two straight lines drawn from the discharge orifice to cut the spray contours at a specified distance from the atomizer face (Rashad et al., 2016). Taking the symmetry of the spray, we will obtain the spray half cone angle. The spray angle is affected by the atomizer nozzle shape and size, spray liquid physical properties and spray environmental factors (Zhang et al., 2017). Furthermore, spray cone angles are dependent on the ambient gas pressure because as the ambient pressure increases, the spray cone angles increase too (Song et al., 2018). For simplex swirl atomizer, the increase in fuel viscosity reduces the spray cone angle due to the higher frictional losses in the atomizer (Lefebvre and Wang, 1987). A spill return type atomizer generated a hollow cone spray with only moderate increase in spray cone angle with increasing inlet pressure while simplex nozzle atomizer spray cone angle were found to be highly dependent on fuel injection pressure (Durdina et al., 2014).

An experiment conducted on jatropha-derived alternative aviation fuel sprays (Sivakumar et al., 2016) found that the spray cone angle characteristics for 20/80 Jatropha HRJ/Jet A-1 spray is relatively closer to that of the Jet A-1 spray. However, for a given flow condition, the spray cone angle for 70/30 Jatropha HRJ/Jet A-1 is higher than Jet A-1. This may be resulting from its lower viscosity.

Liquid atomization is a process of changing the liquid into small droplets (Rashid et al., 2012). It is a process where a liquid jet or sheet is disintegrated by the kinetic energy of the liquid (Lefebvre and McDonell, 2017). The development of the jet or sheet and the growth of small disturbances, which eventually lead to disintegration into ligaments and the drops, are also of primary importance in determining the shape and penetration of the resulting spray as well as its characteristics of number density, drop velocity and drop size distributions as functions of time and space (Lefebvre and McDonell, 2017).

In addition, spray penetration is an important parameter for combustor design, size and geometry since it will provide a significant effect on the engine performance and emission (Azami and Savill, 2016). It has been shown that greater liquid fuel viscosity and surface tension slow the breakup and atomization process (Wilkinson et al., 1993, Ejim et al., 2007) which in turn contribute to longer liquid penetration (Kim et al., 2016). The tip penetration increase with time after being injected from the injector and a higher injection pressure promotes this increase (Chen et al., 2013). High initial temperature accelerates evaporation rate which also reduced the droplet particle's velocity much faster and resulted in a low penetration length (Azami and Savill, 2016). Most liquids become less viscous as the temperature is raised (Wright, 1977). It is reported that higher viscosity fuels have a

lower spray cone angle and higher drop size and spray penetration (Peterson and Auid, 1991).

An experiment on spray characteristics of ethanol-aviation kerosene blended fuel (Song et al., 2018) found that the penetration of the spray decreases with the increasing of ethanol proportion in the blended fuel and the percentage of ethanol mixing can improve the atomization property of blended fuels. A computational work that was conducted by Azami and Savill found that methanol droplet particle propagates the farthest distance and is followed by ethanol, and kerosene fuels (Azami and Savill, 2016). They also found that all biofuels have shorter penetration length in the given time.

The combustion chamber is divided into three zones which are primary zone, secondary zone and dilution zone. It is necessary to verify if there is enough air to enter through every combustion chamber zone holes (Mark and Selwyn, 2016). The need of the liner holes is to provide enough air for complete combustion (Chaudhari et al., 2012). In order to limit the exit gas temperature to be within the required value, to protect the liner walls and to obtain good ignition characteristics coupled with high combustion efficiency at low power conditions, the equivalence ratio in primary zone of combustion chamber entails a range of values in order of 0.7 to 0.95 (Abolgasem Mesoad Alarami, 2015).

# CHAPTER 3

## METHODOLOGY

This chapter describes in details on how the study is conducted. The combustion chamber configuration, the properties of the fuel that are used for the simulation, the formulae that are used to calculate properties of alternative-kerosene fuel mixture, the meshing of the combustion chamber, the CFD modeling, boundary conditions, CFD solution methods, controls, initialization, calculation and the validation for the simulation are further described.

### 3.1 Flow Chart

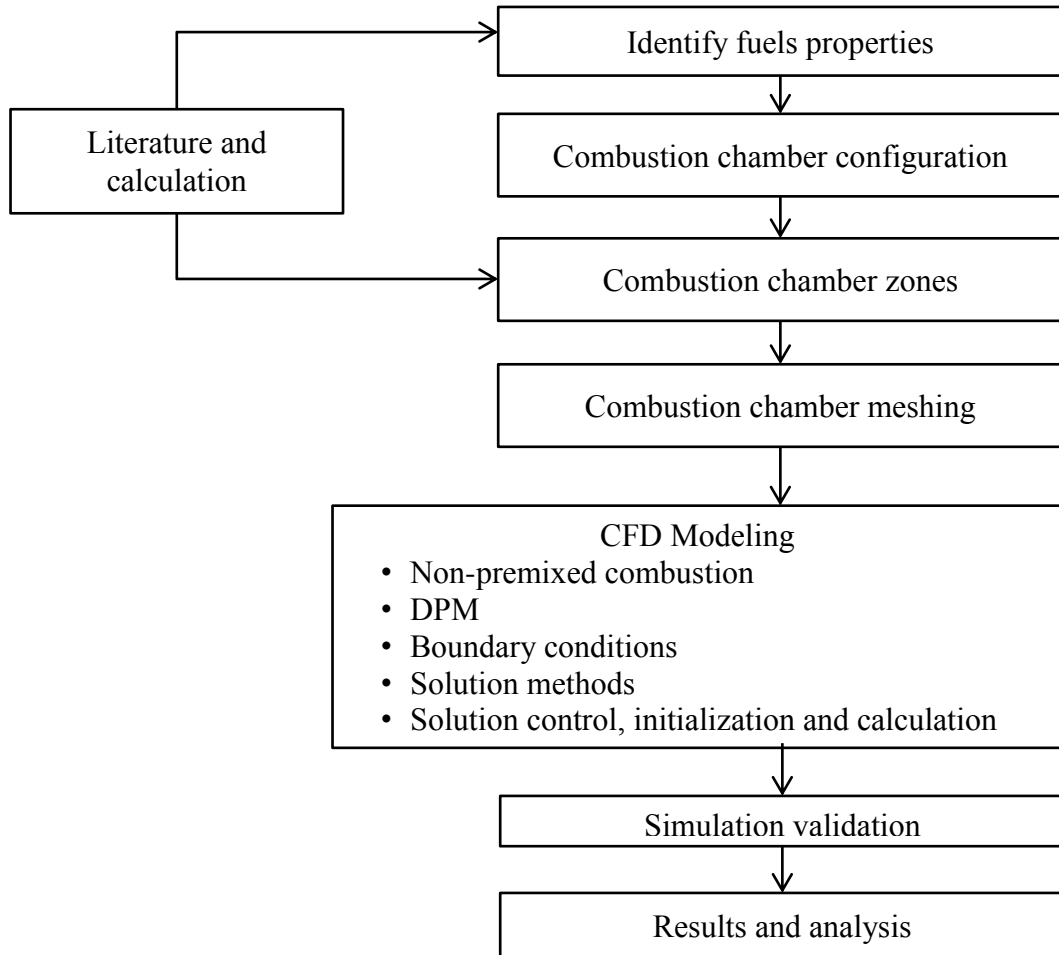


Figure 3.1: Methodology flowchart

### 3.2 Fuels Properties

The fuels that are used for this simulation are Jet-A, JSPK, CSPK, 50JSPK/50Jet-A and 50CSPK/50Jet-A. Table 3.1 shows the fuel properties used in the simulation.

Table 3.1: Fuel properties (Mazlan, 2012, Azami and Savill, 2016).

	<b>Jet-A</b>	<b>JSPK</b>	<b>CSPK</b>	<b>50JSPK/ 50Jet-A</b>	<b>50CSPK/ 50Jet-A</b>
<b>Latent Heat</b> (kJ/kg)	226	251	251	238.5	238.5
<b>Specific Heat, <math>c_p</math></b> (J/kgK)	2093	2010	2010	2051.5	2051.5
<b>Density, <math>\rho</math></b> (kg/m <sup>3</sup> )	780	749	753	764.5	766.5
<b>Binary Diffusivity</b> (m <sup>2</sup> /s)	5.198 x 10 <sup>-7</sup>	5.43 x 10 <sup>-7</sup>	5.37 x 10 <sup>-7</sup>	5.314 x 10 <sup>-7</sup>	5.284 x 10 <sup>-7</sup>
<b>Boiling Point</b> (K)	462	512.25	515.15	487.125	488.575
<b>Vapor Temperature</b> (K)	460	510	513.15	485.125	486.575
<b>Vapor Pressure</b> (Pa)	90.12	239.03	252.56	150.51	155.18

In order to get the value for the saturated vapor pressure for every fuel, the following formula is used.

$$P_{sat} = 1886058.95e^{\left(\frac{-4576.45}{T_p}\right)} \quad (3.1)$$

As for the fuel mixtures, density of the mixture is calculated using equation (3.3).

$$\rho_{mix} = \sum \rho_i x_i \quad (3.2)$$

where  $x$  is the percentage of the fuel mixture and  $i$  is the type of fuel. The similar equation is used to calculate other fuel properties as shown in Table 3.1.

### 3.3 Combustion Chamber Configuration

The simulation is done to simulate the flow inside a simple cylindrical chamber that has an inlet at one end and an outlet at the other end. Since a two-dimensional (2D) computer simulation is performed, only the cross section of the chamber is considered. Configuration of combustion chamber used in this study is obtained from a liquid fuel combustion modeling ANSYS Fluent tutorial that is available online (Jafarinaia, 2017). The injection spray of the fuel is set to be at the center of the inlet. The configuration of the combustion chamber is shown in Figure 3.2.

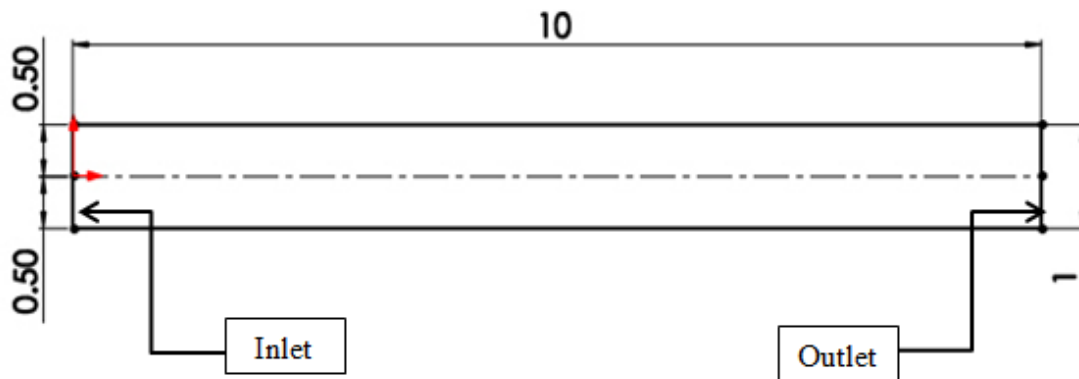


Figure 3.2: Combustion chamber configuration (Jafarinaia, 2017). The dimensions are in meter.

### 3.4 Combustion Chamber Zones

Generally, combustion chamber is divided into three zones; Primary Zone (PZ), Secondary Zone (SZ) and Dilution Zone (DZ). In this study, the chamber has divided into zones based on study conducted by Mark and Selwyn (Mark and Selwyn, 2016) who designed a combustion chamber for turbojet engine. From their study, percent of zone length can be obtained using equation (3.3). Table 3.2 shows zone length and their respective zones length percentage.

$$\text{Zone length \%} = \frac{\text{Zone length}}{\text{Total length}} \times 100 \quad (3.3)$$

Table 3.2: Combustion zones length in the combustion chamber from the journal (Mark and Selwyn, 2016).

<b>Type of Zone</b>	<b>Length (m)</b>	<b>Percentage</b>
Primary Zone	0.03020	25.24 %
Secondary Zone	0.02013	16.82 %
Dilution Zone	0.06933	57.94 %
<b>Total Length</b>	<b>0.11966</b>	<b>100 %</b>

By using the similar equation and the percentage obtained in Table 3.2, the length for every zone for the cylindrical combustion chamber is obtained as shown in Table 3.3.

Table 3.3: Combustion zones length in the combustion chamber for cylindrical combustion chamber.

Type of Zone	Percentage	Length (m)
Primary Zone	25.24 %	2.524
Secondary Zone	16.82 %	1.682
Dilution Zone	57.94 %	5.794
<b>Total Length</b>	<b>100 %</b>	<b>10</b>

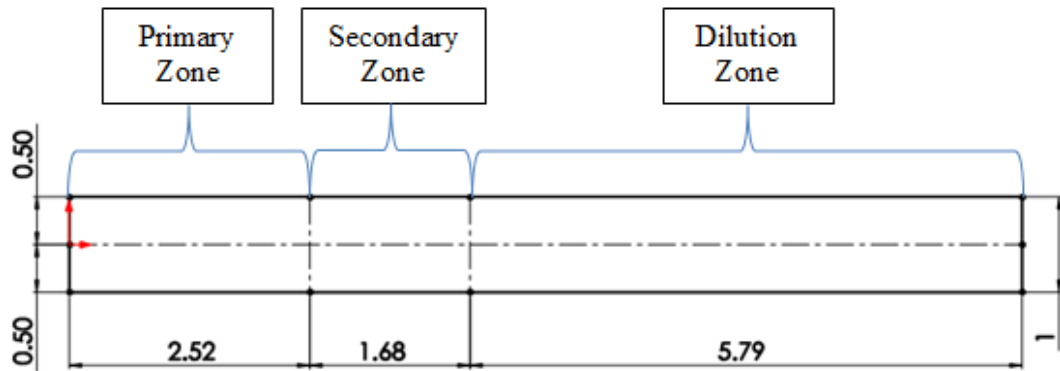


Figure 3.3: Combustion zones for the combustion chamber.

### 3.5 Meshing of the Combustion Chamber

The liquid fuel combustion modeling ANSYS Fluent tutorial included the meshing file for the combustion chamber. The meshing has 5427 of nodes and 5200 quadrilateral cells. The mesh quality for the combustion chamber is shown in Table 3.4.

Table 3.4: Combustion chamber's mesh quality.

<b>Mesh Quality</b>	<b>Value</b>
Minimum Orthogonal Quality	0.9987
Maximum Ortho Skew	0.001332
Aspect Ratio	6.0542

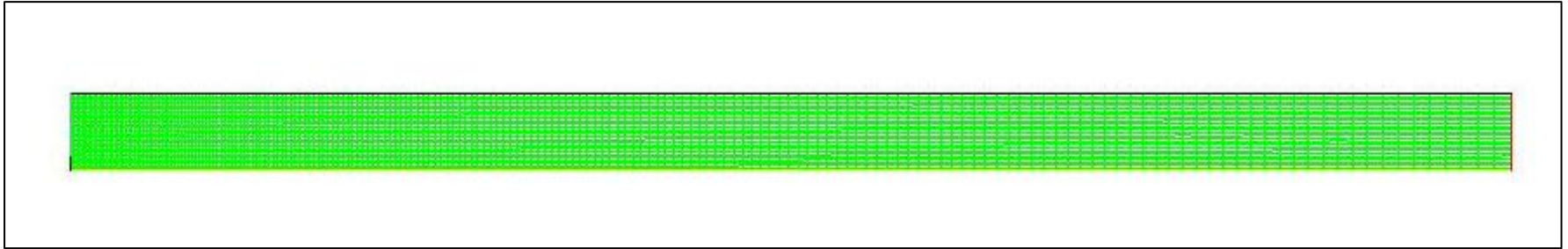


Figure 3.4: Meshing for the half upper part of the combustion chamber.



Figure 3.5: Close up view of the meshing.

### **3.6 CFD Modeling: Non-premixed Combustion**

The simulation was conducted by using ANSYS Fluent software. The viscous model that was used for the simulation was Standard k-epsilon (2eqn) with its default settings. Non-premixed combustion was chosen for the species model. For this non-premixed combustion, non-adiabatic condition is assumed and the operating pressure to be at the ambient pressure which is 101325 Pa. For the boundary species, a new boundary species which is Jet-A,  $C_{12}H_{23}$ , is added. The fuel inlet temperature for liquid fuel combustion is set to be at 294.15K and the oxidizer inlet temperature is set to be at 1000K.

### **3.7 CFD Modeling: Discrete Phase Model**

Discrete Phase Model (DPM) is used to model the flow of liquid droplets. This model predicts the trajectories of individual liquid droplets, each representing a continuous stream (or mass flow) of fuel. Heat, momentum, and mass transfer between the liquid fuel and the air flow are included by alternately computing the discrete phase trajectories and the gas phase continuum equations (Jafarinia, 2017). For this case study, a few assumptions are made to simplify the simulation.

Injection of droplet particle type is set as group with number of streams of 20 is selected. Group injection required the input velocity in X and Y directions. Therefore to evaluate the effect of spray half cone angles,  $\theta$  on combustion characteristics, the velocity in both X and Y directions is obtained by using trigonometry right triangles formula.

$$Y \text{ velocity} = X \text{ velocity} \times \tan \theta \quad (3.4)$$

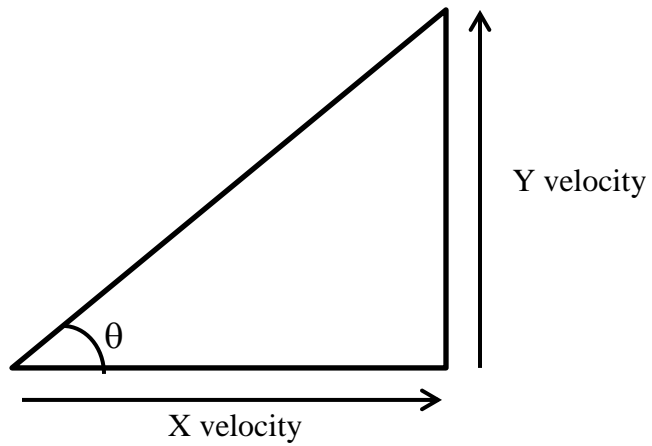


Figure 3.6: Drop velocity representation in X and Y directions.

The velocity of the injection for every spray half cone angle is shown in Table 3.5 .

Table 3.5: X and Y velocity for every spray half cone angle.

<b>Spray Half Cone Angle, <math>\theta</math></b> (°)	<b>X Velocity</b> (m/s)	<b>Y Velocity</b> (m/s)
30	100	57.74
40	100	83.91
50	100	119.18

Since the only variable for injection is the spray half cone angle, the other properties for the particle injection were fixed. Table 3.6 shows the properties for the particle injection.

Table 3.6: Particle injection properties.

Particle Diameter	$20\mu m$
Temperature	300 K
Flow rate	$0.0002\text{ kg/s}$

In turbulent dispersion, Discrete Random Walk model under Stochastic Tracking was enabled. Stochastic tracks model the effect of turbulence in the gas phase on the droplet trajectories. Stochastic tracking is important in liquid fuel combustion simulations to simulate realistic droplet dispersion (Jafarinia, 2017).

### 3.8 Boundary Conditions

For this case study, the combustion chamber has four boundary conditions which are the inlet, outlet, wall and symmetry. Note that the cross section of the combustion chamber is basically a symmetrical rectangle. So, the simulation can be done only for the upper part. This corresponds with the simulation that was done by Oliveira and Brójo which they only did quarter of the geometry (Oliveira and Brójo, 2017). The inlet was set to be a velocity inlet. Table 3.7 below shows the conditions for the inlet boundary.

Table 3.7: Inlet boundary conditions.

Velocity Specification Method	Magnitude and Direction
Velocity Magnitude	1 <i>m/s</i>
Initial Gauge Pressure	0 Pa
Turbulence Specification Method	Intensity and Hydraulic Diameter
Turbulent Intensity	10%
Hydraulic Diameter	2 <i>m</i>
Temperature	1000 K
Discrete Phase BC Type	Escape

For the outlet boundary, it is set to be pressure outlet. Table 3.8 shows the conditions set up for the outlet boundary.

Table 3.8: Outlet boundary conditions.

Backflow Reference Frame	Absolute
Gauge Pressure	0 Pa
Backflow Pressure Specification Method	Normal to Boundary
Turbulence Specification Method	Intensity and Hydraulic Diameter
Turbulent Intensity	10%
Hydraulic Diameter	2 <i>m</i>
Temperature	1800 K
Discrete Phase BC Type	Escape

Another important boundary condition for this case study is the wall. Table 3.9 shows the conditions that were set up for the wall boundary.

Table 3.9: Wall boundary conditions.

Wall Motion	Stationary Wall
Shear Condition	No Slip
Wall Roughness	Standard
Temperature Thermal Conditions	1200 K
Discrete Phase Model Conditions	Reflect

### **3.9 CFD Solution Methods**

The pressure-velocity coupling scheme that was chosen for this case study is SIMPLE. Default settings are used for the spatial discretization except for pressure, turbulent kinetic energy and turbulent dissipation rate which were changed to second order upwind.

### **3.10 CFD Solution Control, Initialization and Calculation**

Under the solution controls, the under-relaxation factors are all set to default. Hybrid initialization is used for all the simulations and 500 iterations of calculation were set for every spray half cone angle and for every fuel type.